

Supporting Information

Reduced Open-Circuit Voltage Loss for Highly Efficient Low-Bandgap Perovskite Solar Cells via Suppression of Silver Diffusion

Meiyue Liu,^{1†} Ziming Chen,^{1†} Yongchao Yang,¹ Hin-Lap Yip^{1,2} and Yong Cao¹

¹ State Key Laboratory of Luminescent Materials and Devices, Institute of Polymer Optoelectronic Materials and Devices, School of Materials Science and Engineering, South China University of Technology, 381 Wushan Road, Guangzhou, 510640, P. R. China.

² Innovation Center for Printed Photovoltaics, South China Institute of Collaborative Innovation, Dongguan 523808, P. R. China

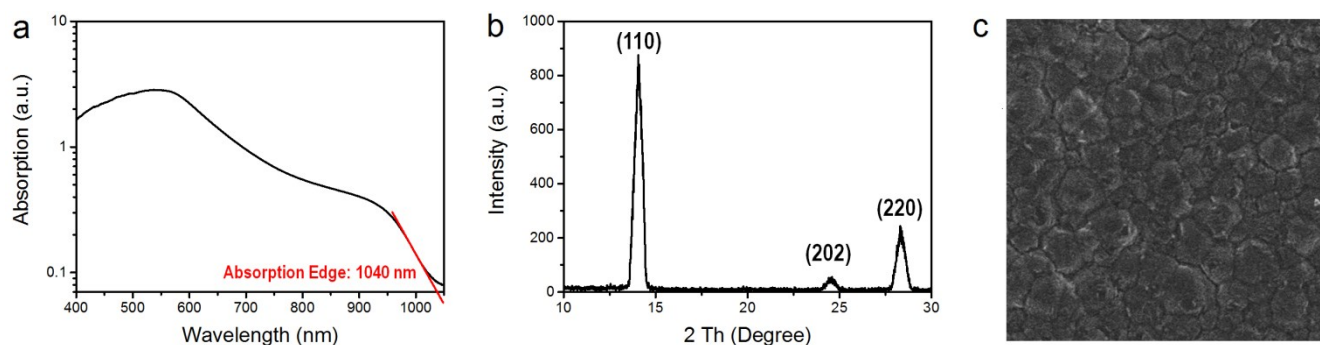


Figure S1. (a) Absorption spectrum of $\text{FA}_{0.5}\text{MA}_{0.5}\text{Sn}_{0.5}\text{Pb}_{0.5}\text{I}_3$ film. (b) XRD pattern of $\text{FA}_{0.5}\text{MA}_{0.5}\text{Sn}_{0.5}\text{Pb}_{0.5}\text{I}_3$ film. (c) SEM image of $\text{FA}_{0.5}\text{MA}_{0.5}\text{Sn}_{0.5}\text{Pb}_{0.5}\text{I}_3$ film above PEDOT:PSS layer. The size of this area is $4 \times 4 \mu\text{m}^2$.

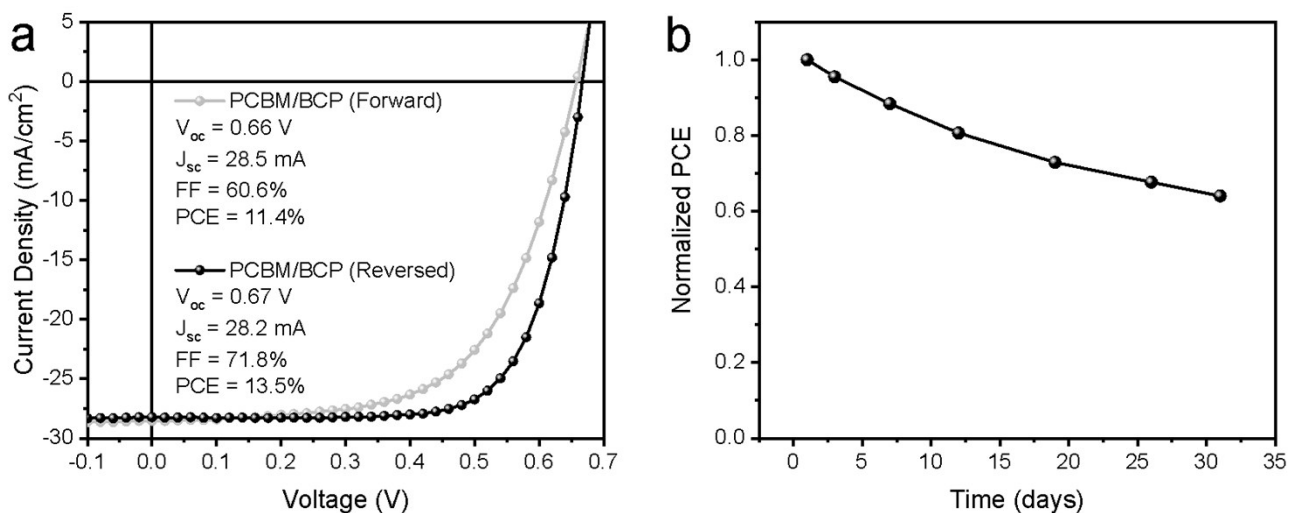


Figure S2. (a) J-V curves and (b) stability of perovskite solar cells with PCBM/BCP ETL.

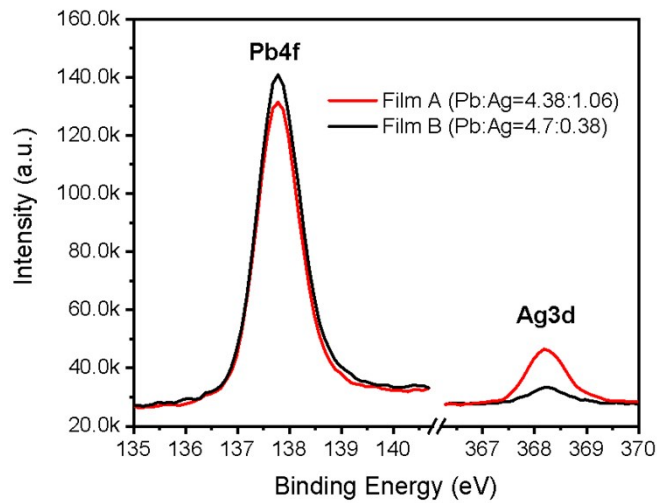


Figure S3. XPS data of Pb4f and Ag3d signal in Film A and Film B. The atomic ratio of Pb4f in Film A and Film B is 4.38% and 4.7%, respectively; the atomic ratio of Ag3d signal in Film A and Film B is 1.06% and 0.38%, respectively, suggesting a much smaller Pb to Ag ratio in Film A.

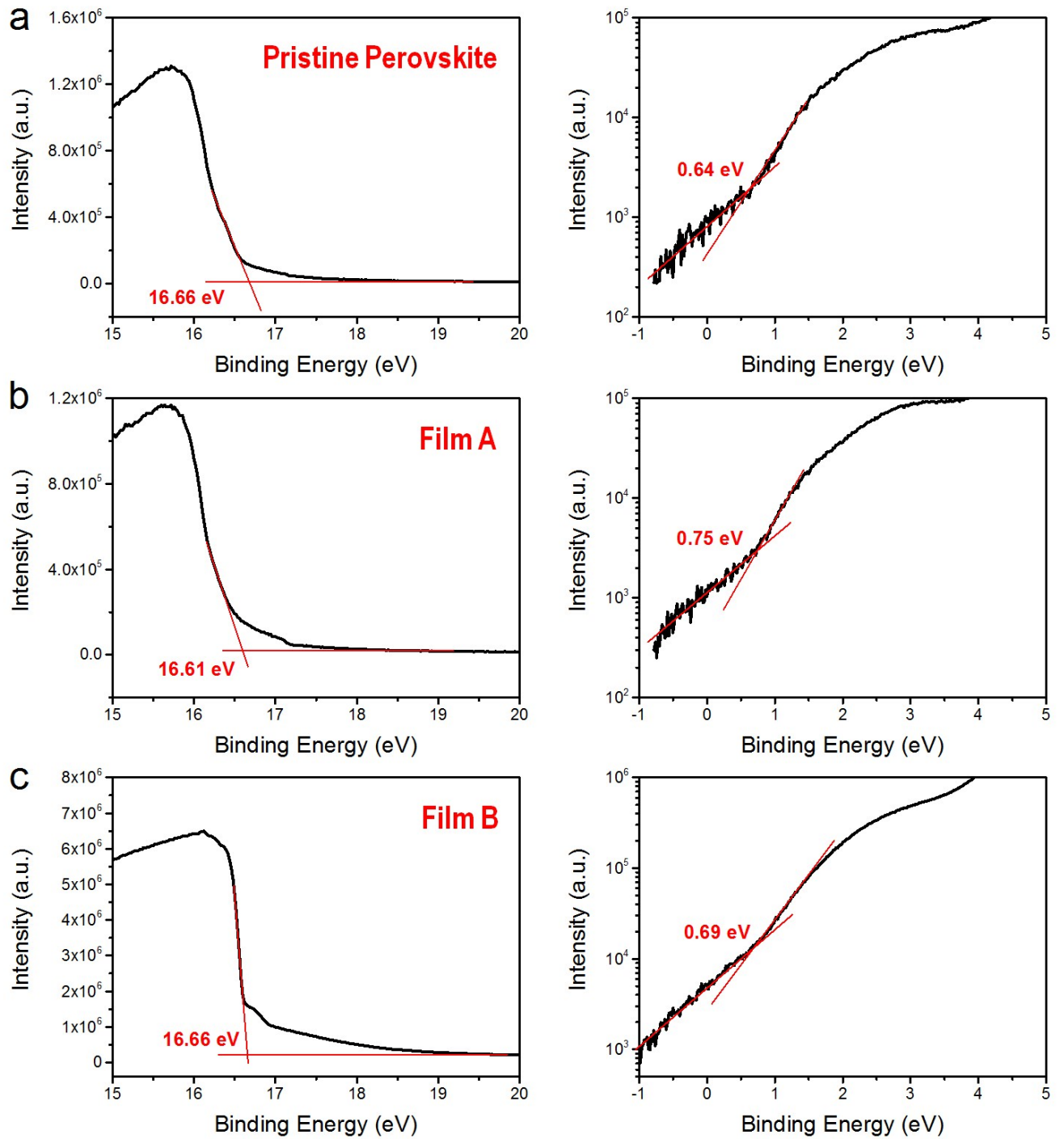


Figure S4. UPS spectra of $\text{FA}_{0.5}\text{MA}_{0.5}\text{Sn}_{0.5}\text{Pb}_{0.5}\text{I}_3$ perovskite films. In the UPS measurements, a He I source with photon energy of 21.22 eV was used to excite the sample. Therefore, the calculated valence bands for (a) pristine perovskite, (b) Film A and (c) Film B are 5.20 eV, 5.36 eV and 5.25 eV, respectively.

Table S1. Photovoltaic parameters of perovskite solar cells with various PCBM thicknesses.

PCBM thickness (nm)	V_{oc} (V)	J_{sc} (mA/cm ²)	FF (%)	PCE (%)
0	0.22	20.5	56.7	2.5
15	0.33	29.1	63.1	6.0
35	0.43	29.5	52.8	7.3
50	0.55	27.4	66.7	9.7
70	0.59	28.8	64.6	11.0
100	0.63	29.7	63.7	12.0
130	0.64	29.2	65.8	12.4
160	0.66	27.8	68.3	12.5
190	0.69	25.5	70.5	12.4

Table S2. A summary of PCE and V_{oc} loss of low-bandgap PVSCs based on published reports.

Perovskite	Bandgap (eV)	V_{oc} (V)	V_{oc} loss (V)	PCE (%)	Ref.
MASn _{0.5} Pb _{0.5} I ₃	1.17	0.584	0.586	7.27	S1
FASn _{0.5} Pb _{0.5} I ₃	1.28	0.695	0.585	10.76	S2
MASn _{0.25} Pb _{0.75} I ₃	1.3	0.73	0.57	15.2	S3
FA _{0.5} MA _{0.5} Sn _{0.5} Pb _{0.5} I ₃	1.3	0.78	0.52	14.2	S4
FA _{0.5} MA _{0.5} Sn _{0.5} Pb _{0.5} I ₃ +AA	1.3	0.78	0.52	14.01	S5
FAPb _{0.7} Sn _{0.3} I ₃ +MASCN	1.28	0.78	0.5	16.26	S6
MASn _{0.5} Pb _{0.5} I _x Cl _{3-x}	1.19	0.70	0.49	12.3	S7
MASn _{0.5} Pb _{0.5} I _x Cl _{3-x} + NAP	1.19	0.71	0.48	13.4	S8
MASn _{0.5} Pb _{0.5} I ₃	1.2	0.75	0.45	13.6	S9
FA _{0.5} MA _{0.5} Sn _{0.5} Pb _{0.5} I ₃	1.2	0.75	0.45	17.6	S10
(FASnI ₃) _{0.6} (MAPbI ₃) _{0.4} +GuaSCN	1.25	0.834	0.416	20.5	S11
(FASnI ₃) _{0.6} (MAPbI ₃) _{0.4}	1.2	0.795	0.405	15.08	S12
(FASnI ₃) _{0.6} (MAPbI ₃) _{0.4}	1.25	0.85	0.4	17.6	S13
FA_{0.5}MA_{0.5}Sn_{0.5}Pb_{0.5}I₃ + SnF₂ + Pb(SCN)₂	1.19	0.79	0.4	18.1	Our Work
(FASnI ₃) _{0.6} (MAPbI ₃) _{0.4} +PBDB-T:ITIC	1.25	0.86	0.39	18.03	S14
(FASnI ₃) _{0.6} (MAPbI ₃) _{0.4} +Br	1.272	0.888	0.384	19.03	S15

Supplementary References:

[S1] F. Hao, C. C. Stoumpos, R. P. H. Chang and M. G. Kanatzidis, Anomalous band gap behavior in mixed Sn and Pb perovskites enables broadening of absorption spectrum in solar cells, *J. Am. Chem. Soc.*, 2014, **136**, 8094-8099.

- [S2] J. Liu, G. Wang, Z. Song, X. He, K. Luo, Q. Ye, C. Liao and J. Mei, FAPb_{1-x}Sn_xI₃ mixed metal halide perovskites with improved light harvesting and stability for efficient planar heterojunction solar cells, *J. Mater. Chem. A*, 2017, **5**, 9097-9106.
- [S3] H. L. Zhu, J. Xiao, J. Mao, H. Zhang, Y. Zhao and W. C. H. Choy, Controllable Crystallization of CH₃NH₃Sn_{0.25}Pb_{0.75}I₃ Perovskites for Hysteresis-Free Solar Cells with Efficiency Reaching 15.2%, *Adv. Funct. Mater.*, 2017, **27**, 1605469.
- [S4] Z. Yang, A. Rajagopal, C.-C. Chueh, S. B. Jo, B. Liu, T. Zhao and A. K.-Y. Jen, Stable low-bandgap Pb-Sn binary perovskites for tandem solar cells, *Adv. Mater.*, 2016, **28**, 8990-8997.
- [S5] X. Xu, C.-C. Chueh, Z. Yang, A. Rajagopal, J. Xu, S. B. Jo and A. K.-Y. Jen, Ascorbic acid as an effective antioxidant additive to enhance the efficiency and stability of Pb/Sn-based binary perovskite solar cells, *Nano Energy*, 2017, **34**, 392-398.
- [S6] X. Lian, J. Chen, Y. Zhang, M. Qin, J. Li, S. Tian, W. Yang, X. Lu, G. Wu and H. Chen, Highly Efficient Sn/Pb Binary Perovskite Solar Cell via Precursor Engineering: A Two-Step Fabrication Process, *Adv. Funct. Mater.*, 2018, **29**, 1807024.
- [S7] M. Liu, Z. Chen, Q. Xue, S. H. Cheung, S. K. So, H.-L. Yip and Y. Cao, High performance low-bandgap perovskite solar cells based on a high-quality mixed Sn-Pb perovskite film prepared by vacuum-assisted thermal annealing, *J. Mater. Chem. A*, 2018, **6**, 16347-16354.
- [S8] Z. Chen, M. Liu, Z. Li, T. Shi, Y. Yang, H.-L. Yip and Y. Cao, Stable Sn/Pb-based perovskite solar cells with a coherent 2D/3D interface, *iScience*, 2018, **9**, 337-346.
- [S9] Y. Li, W. Sun, W. Yan, S. Ye, H. Rao, H. Peng, Z. Zhao, Z. Bian, Z. Liu, H. Zhou and C. Huang, 50% Sn-based planar perovskite solar cell with power conversion efficiency up to 13.6%, *Adv. Energy Mater.*, 2016, **6**, 1601353.
- [S10] G. Kapil, T. S. Ripolles, K. Hamada, Y. Ogomi, T. Bessho, T. Kinoshita, J. Chantana, K. Yoshino, Q. Shen, T. Toyoda, T. Minemoto, T. N. Murakami, H. Segawa and S. Hayase, Highly efficient 17.6% tin-lead mixed perovskite solar cells realized through spike structure, *Nano Lett.*, 2018, **18**, 3600-3607.
- [S11] J. Tong, Z. Song, D. H. Kim, X. Chen, C. Chen, A. F. Palmstrom, P. F. Ndione, M. O. Reese, S. P. Dunfield, O. G. Reid, J. Liu, F. Zhang, S. P. Harvey, Z. Li, S. T. Christensen, G. Teeter, D. Zhao, M. M. Al-Jassim, M. F. A. M. v. Hest, M. C. Beard, S. E. Shaheen, J. J. Berry, Y. Yan and K. Zhu, Carrier lifetimes of >1 μs in Sn-Pb perovskites enable efficient all-

perovskite tandem solar cells, *Science*, 2019, DOI: 10.1126/science.aav7911.

[S12] W. Liao, D. Zhao, Y. Yu, N. Shrestha, K. Ghimire, C. R. Grice, C. Wang, Y. Xiao, A. J. Cimaroli, R. J. Ellingson, N. J. Podraza, K. Zhu, R.-G. Xiong and Y. Yan, Fabrication of efficient low-bandgap perovskite solar cells by combining formamidinium tin iodide with methylammonium lead iodide, *J. Am. Chem. Soc.*, 2016, **138**, 12360-12363.

[S13] D. Zhao, Y. Yu, C. Wang, W. Liao, N. Shrestha, C. R. Grice, A. J. Cimaroli, L. Guan, R. J. Ellingson, K. Zhu, X. Zhao, R.-G. Xiong and Y. Yan, Low-bandgap mixed tin-lead iodide perovskite absorbers with long carrier lifetimes for all-perovskite tandem solar cells, *Nat. Energy*, 2017, **2**, 17018.

[S14] G. Xu, P. Bi, S. Wang, R. Xue, J. Zhang, H. Chen, W. Chen, X. Hao, Y. Li and Y. Li, Integrating ultrathin bulk-heterojunction organic semiconductor intermediary for high-performance low-bandgap perovskite solar cells with low energy loss, *Adv. Funct. Mater.*, 2018, **28**, 1804427.

[S15] C. Li, Z. Song, D. Zhao, C. Xiao, B. Subedi, N. Shrestha, M. M. Junda, C. Wang, C.-S. Jiang, M. Al-Jassim, R. J. Ellingson, N. J. Podraza, K. Zhu, and Y. Yan, Reducing saturation-current density to realize high efficiency low-bandgap mixed tin-lead halide perovskite solar cells, *Adv. Energy Mater.*, 2018, **9**, 1803135.